

# Modelling and Development of Multisectional Disk Piezoelectric Transducers for Critical Application Systems

Ibrahim M. Aladwan<sup>1</sup>, Constantine Bazilo<sup>2</sup>, Emil Faure<sup>2\*</sup>

<sup>1</sup>*Al-Balqa' Applied University, Amman, Jordan*

<sup>2</sup>*Cherkasy State Technological University, Cherkasy, Ukraine*

Received 13 JUNE 2021

Accepted 30 JAN 2022

## Abstract

The accuracy and reliability of computer systems largely depend on the characteristics of the transducers. The main advantage of using multisectional piezoceramic transducers is their special structure that makes it possible to implement fundamentally different circuits in such one element with a simultaneous increase in the degree of integration and hybridization of their operational properties. Diversity and variation of practical applications of piezoelectric transducers and devices on their bases naturally stimulate their theoretical research. Because of the absence of reliable and valid methods of constructing mathematical models of multisectional piezoelectric transducers, it is essential to consider the excitation of oscillations in transducers with group inclusion of sections taking into account the acoustic feedback. The paper considers the development of the mathematical model of a multisectional disk piezoelectric transducer taking into account the acoustic feedback that exists between the area under the electrode of the primary electrical circuit and all, without exception, the areas located under the electrodes of the secondary circuits. Proposed scheme maintains its logical structure in the wide range of the number of sections. The features of constructing mathematical models of multisectional transducers that arise when the sections are switched on in groups are considered. Based on the modelling, the methods for modifying disk piezoelectric transducers using a polyelectrode design, technology of additional elements, the spatial power structure of piezoelectric transducers, and physical models of transducers based on multisectional piezoelectric disks with improved characteristics, are described. The designs of a multifunctional piezoelectric transducer in the volume of one body are proposed.

© 2022 Jordan Journal of Mechanical and Industrial Engineering. All rights reserved

**Keywords:** piezoelectric disk, multifunctional transducer, physical processes, mathematical description, critical systems.

## 1. Introduction

The stable operation of computer systems, especially of critical application, largely depends on the reliability of the functioning of such computer systems. The most important part in this issue is the reliability of the functioning of both software and hardware of computer systems [1].

The integral elements of the hardware of computer systems regarding the characteristics of which the accuracy and reliability of their operation largely depend, are transducers [2].

Automatic space stations, autonomous deep-sea floating objects, and any other objects, access to which is very difficult, impossible or extremely dangerous for humans, such as (nuclear reactors, chemically hazardous objects, underground objects, orbiting satellites, etc.) are among the computer systems of critical application where high reliability, stability, autonomy, maximum uptime of such ultra-reliable transducers are required [3], [4].

The block diagram of the location of the sensors in the computer system on the example of a data collection and management system [5] is shown in Figure 1. Different material objects, such as cars, spaceships, human bodies, various liquids and gases can be the subjects of measurements. Data about the measured object is collected by sensors, some of which (2, 3 and 4) are located on the surface or inside the object. Sensor 1 has no direct

connection with the object, i.e. is contactless. Sensor 5 can perform various functions. It often serves to control conditions within the data collection system itself.

Many modern systems have to be built into rather miniature devices. Very often the geometry of the printed circuit board of a system is determined by the case of the device for which it is intended. Therefore, the miniaturization of execution is one of the problems of the developer of modern systems [6].

The main advantage of using transducers from piezoceramic materials [7], [8] with separated electrodes in computer systems is determined by their special structure. This makes it possible to implement fundamentally different circuits in one such element, with a simultaneous increase in the degree of integration and hybridization of their operational properties [9].

Diversity and variation of practical applications of piezoelectric transducers and devices on their bases naturally stimulate their theoretical research.

As some studies have shown, transducers based on multisectional disk piezoceramic elements, have a number of advantages [3]. Some principles of constructing a mathematical model of disk piezoelectric transducers are given in works [10], [11]. However, based on the analysis of literary sources [12], [13] it was determined that at present there are no methods for constructing mathematical models of multisectional piezoelectric transducers for computer systems of critical application.

\* Corresponding author e-mail: faureemilr@gmail.com.

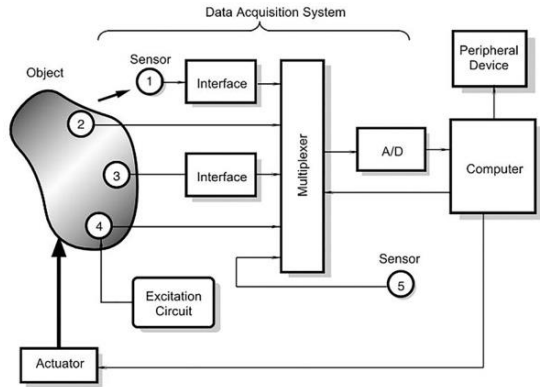


**Figure 1.** Location of sensors in the data collection system. Sensor 1 is non-contact, sensors 2 and 3 are passive, sensor 4 is active, and sensor 5 is built into the data collection system [5]

The aim of the paper is to construct a mathematical model of multisectional piezoceramic disk transducers and to develop examples of multisectional transducers with improved characteristics.

**2. Materials and methods**

Consider a piezoelectric disk transducer with separated electrodes, which has two or more secondary electrical circuits. In what follows, such transducers will be called multisectional or polyelectrode.

Figure 2 schematically depicts a disk transducer with three ring electrodes in secondary electrical circuits. The electrode of the primary electrical circuit has the shape of a circle with a radius  $R_1^{(2)}$ . A source of electrical potential difference  $U_0 e^{i\omega t}$  is connected to it ( $U_0$  is an amplitude of electrical potential difference;  $i = \sqrt{-1}$  is an imaginary unit;  $\omega$  is a circular frequency;  $t$  is a time).

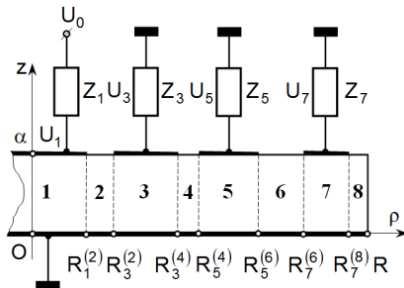


**Figure 2.** Design diagram of a multisectional piezoelectric transducer with three secondary electric circuits

The output impedance of the source of electrical potentials is indicated by the symbol  $Z_1$ . The symbols  $Z_3, \dots, Z_7$  indicate the electrical impedances of the loads in the secondary electrical circuits of the transducer. A piezoelectric disk element is made of PZT type material. The bottom surface ( $z=0$ ) of the disk is completely electroded [14] and grounded.  $R_{2n+1}^{(2n)}$  and  $R_{2n+1}^{(2n+2)}$  are left and right boundaries of the circular area under the electrode of the  $(2n+1)$ -th number,  $\alpha$  is a disk thickness.

In some cases, it turns out to be advisable to group inclusion of sections of a multisectional disk piezoelectric transducer [3]. Consider the features of calculating the transformation ratios that arise in these situations (Fig. 3).

Figure 3, schematically shows four-sectional piezoelectric transducer, two electrodes of which are included in the primary electrical circuit. Such an inclusion allows, in principle, to increase the power of signals in secondary electrical circuits. The other two ring electrodes are included in two different secondary electrical circuits.

The mathematical model of the multisectional piezoelectric transducer (Fig. 3, a) can be written as follows:

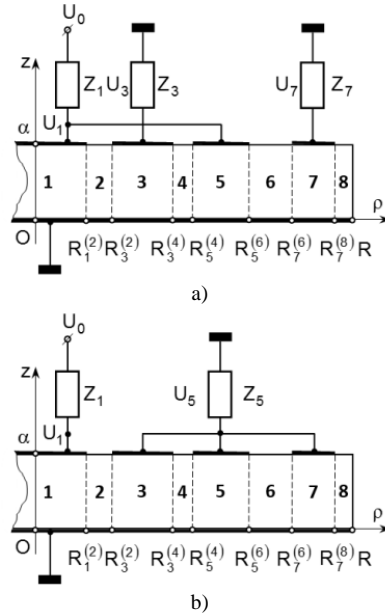


**Figure 3.** Design diagrams of multisectional piezoelectric transducers with group inclusions of sections

$$K_{2n+1}(\omega) = \frac{\Psi_{2n+1}(k, R)}{1 - i\omega C_1^* Z_1 \left\{ \Psi_1(k, R) - 1 + \left( C_5^* / C_1^* \right) \left[ \Psi_5(k, R) - 1 \right] \right\}} \quad (1)$$

( $n = 1; 3$ ),

where frequency-dependent dimensionless functions  $\Psi_1(k, R)$ ,  $\Psi_3(k, R)$ ,  $\Psi_5(k, R)$  and  $\Psi_7(k, R)$  are defined in Appendix A;  $C_1^*$  and  $C_5^*$  are the electrical capacities of the disk areas under electrodes 1 and 5, respectively;  $k$  is a wave number of radial oscillations in the  $(2n+1)$ -th area under the corresponding electrode.

Figure 3, b schematically shows a disk transducer with three ring electrodes in secondary electrical circuits. The electrode of the primary electric circuit has the disk shape with radius  $R_1^{(2)}$ . The source of the difference of electric potentials  $U_0 e^{i\omega t}$  is connected to it. The output resistance of the source of electric potentials is indicated by a symbol  $Z_1$ . The symbol  $Z_5$  indicates the electrical load impedance in the secondary electrical circuit of piezoelectric transducer.

The mathematical model of the multisectional piezoelectric transducer (Fig. 3, b) can be written as follows:

$$K_5(\omega) = - \frac{\Psi_5(k, R)}{1 - i\omega C_1^* U_1 \left[ \Psi_1(k, R) - 1 \right]} \quad (2)$$

where frequency-dependent dimensionless functions  $\Psi_1(k, R)$  and  $\Psi_5(k, R)$  are defined in Appendix B.

Expression (2) differs from all known results obtained by other authors in that it is constructed taking into account the acoustic feedback that exists between the area under the electrode of the primary electrical circuit and all, without exception, the areas located under the electrodes of the secondary circuits.

### 3. Modelling

It is obvious that the features of the change in the electrical impedance of the piezoelectric transducer are due to the change in the characteristics of the stress-strain state of the disk. Indeed, the electric current collected by the electroded surfaces  $z = \pm a/2$  ( $a$  is a piezoelectric disk thickness) of the oscillating disk has an amplitude

$$I = -\omega \int_S D_z dS = \int_S [e_{3k1} \varepsilon_{k1} + \chi_3^e E_z] dS, \quad (3)$$

where  $D_z$  is an axial component of the electric induction vector;  $S$  and  $dS$  are area and area element of the electroded disk surface;  $e_{3k1}$  is a component of the tensor of piezoelectric constants (piezomodules);  $\varepsilon_{k1}$  is an elastic tensor component;  $\chi_3^e$  is a component of the diagonal tensor of dielectric permittivity of the "clamped" sample;  $E_z$  is a component of the electric field strength vector in the volume of the deformable piezoelectric.

From the general relation (3) it clearly follows that the amplitude value of the current  $I$  and, therefore, the value  $Z_{el}(\omega)$  are determined by the stress-strain state of the plate at a given frequency (values  $\varepsilon_{k1}$  and  $E_z$ ) and a set of material constants (values  $e_{3k1}$  and  $\chi_3^e$ ). Since the deformations  $e_{3k1}$  are determined by the values of the elastic modules, it can be concluded that the analytical description of the electrical impedance of an oscillating piezoceramic disk contains the entire set of physical and mechanical parameters of piezoelectric ceramics. This

circumstance unambiguously indicates that, through the study of the features of the frequency-dependent behavior of the electrical impedance of the sample under study, one can come to the determination of the numerical values of the physical and mechanical parameters of the piezoelectric ceramics from which this sample is made.

Figure 4 shows a graph of the impedance frequency-dependent change of the disk made of PZT piezoelectric ceramics, which fluctuates in the air. The characteristic clearly shows singular points at which the modulus of electrical impedance acquires local minima and maxima. The inset in Fig. 4 shows the change in the modulus of electrical impedance near the frequency of the first local minimum. In the calculations, the following parameters were taken: the radius of piezoceramic disk  $R = 33 \cdot 10^{-3}$  m; the thickness  $a = 3 \cdot 10^{-3}$  m; the disk material parameters [15], [16]:  $c_{11}^E = 110$  GPa;  $c_{12}^E = 60$  GPa;  $c_{33}^E = 100$  GPa;  $e_{33} = 18$  C/m<sup>2</sup>;  $e_{31} = -8$  C/m<sup>2</sup> and  $\chi_{33}^e = 1400 \chi_0$ ;  $Q_M = 100$ ;  $k = c_{12}/c_{11} = 0,324$ . The ordinate shows the values of the modulus of electrical impedance in kilohms, the abscissa shows the dimensionless frequency  $\Omega = \lambda R = \omega \tau_0$ , where  $\tau_0 = R/v$ ;

$v = \sqrt{c_{11}/\rho_0}$  is a speed of propagation of elastic vibrations in a thin disk. For the above parameter values  $v = 3162$  m/s and  $\tau_0 = 10,44 \cdot 10^{-6}$  s. The value  $\Omega = \lambda R = 1$  corresponds to the frequency  $f = 15,25$  kHz. The calculations were performed at the frequencies of the first two electromechanical resonances.

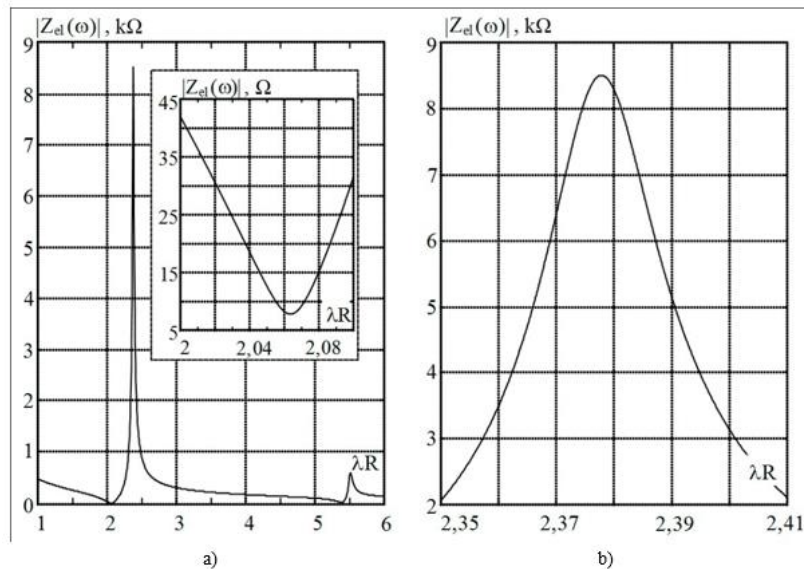


Figure 4. Disk electrical impedance modulus in mid-frequency

At the frequency of resonant energy consumption, an infinite (in amplitude) displacement current can flow through a piezoelectric disk from an ideal (lossless) piezoelectric. Infinite currents with a finite difference in electrical potentials correspond to zero values of electrical resistance. For this reason, at the frequency of electromechanical resonance (the frequency at which the resonant energy consumption of the oscillation source occurs), the electrical impedance of a disk from an ideal piezoelectric is zero. In a real piezoelectric, there are always certain losses of the energy supplied to it, and therefore, at the frequency of electromechanical resonance, the modulus  $Z_{el}(\omega)$  reaches a minimum, but not zero, value. The inset in Fig. 4 shows this clearly.

At the frequency when the modulus  $Z_{el}(\omega)$  reaches a local maximum, the electric current in the conductors that are connected to the electroded surfaces of the oscillating disk vanishes. Zero electric current at finite values of the electrical potential difference corresponds to an infinite electrical resistance, i.e., an open circuit. In a real piezoelectric, there are always losses (leaks), it has a finite electrical conductivity, therefore, at the frequencies of electromechanical antiresonance,  $Z_{el}(\omega)$  reaches maximum, but finite, values [3].

In a real experiment, zeros and infinities are absent, since in real elastic materials there are always losses due to viscous friction. These losses can be taken into account using a parameter  $Q_m$  that makes sense to the mechanical quality factor of the material. As it is known, the quality factor is a dimensionless number, the value of which is inversely proportional to the energy losses in the oscillatory system over the period. In ideal elastic bodies, where there are no energy losses due to viscous friction,  $Q_m \rightarrow \infty$ . In real objects, the quality factor  $Q_m$  has a finite value.

**4. Experiments**

The block diagram of the laboratory model, which is used to determine the material constants of piezoelectric ceramics, is shown in Fig. 5.

A harmonic signal generator (HSG) generates an electrical potential difference  $U_0 e^{i\omega t}$ , the frequency of the change of sign of which is controlled by an electronic frequency meter (EFM).

Keys K1 and K2 are designed for more accurate measurement of the frequency of electromechanical resonance (key K1 is open, and key K2 is closed) and antiresonance (key K1 is closed, and key K2 is open). In the first case, the electronic voltmeter EV1 measures the voltage drop  $U_1$  at a low impedance  $|Z_{el}(\omega)|$  and therefore its sensitivity is set as high as possible. In the second case, when the key K2 is opened, the situation is repeated. The voltmeter EV2 measures the voltage drop across the resistor  $R_2$ , the value of which is selected from the condition of the inequality  $R_2 \ll |Z_{el}(\omega_a)|$ , where  $\omega_a$  is an electromechanical anti-resonance frequency, and the voltmeter EV2 sensitivity is set as high as possible. The frequencies of resonances and anti-resonances are reliably determined from changes in the readings of voltmeters tuned to the maximum sensitivity [16].

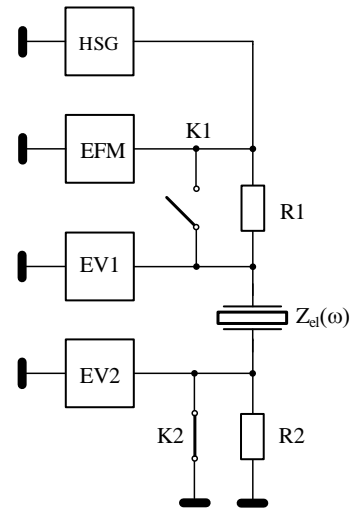


**Figure 5.** Circuit of experimental determination of the frequencies of electromechanical resonances and antiresonances of oscillations of a piezoceramic disk and calculation of the basic material constants of piezoelectric ceramics from their values

The electrical impedance  $Z_{el}(\omega)$  of piezoceramic disk (Fig. 5), elastic vibrations in which are excited by the action of an external electric potential difference, is determined by Ohm's law for a section of the circuit,

$$Z_{el}(\omega) = \frac{U_{el}}{I}, \quad (4)$$

where  $I$  is an amplitude value of current in electric circuit.

The electrical impedance modulus of the oscillating sample  $|Z_{el}(\omega)| = \frac{U_1 R_1}{(U_0 - U_1)}$  is determined from the

voltage drop  $U_1$  across the test sample  $Z_{el}(\omega)$  measured by electronic voltmeter EV1 and from the known value of  $U_0$ . When measured with an EV2 voltmeter, the calculation formula for the modulus of electrical impedance has a

$$\text{slightly different form } |Z_{el}(\omega)| = \frac{(U_0 - U_2) R_2}{U_2}.$$

A disk piezoelectric element  $\varnothing 66 \times 3$  mm made of PZT type material is used for experimental studies.

The results of measuring the electrical impedance of the piezoelectric disk in the mid-frequency area are shown in Figure 6.

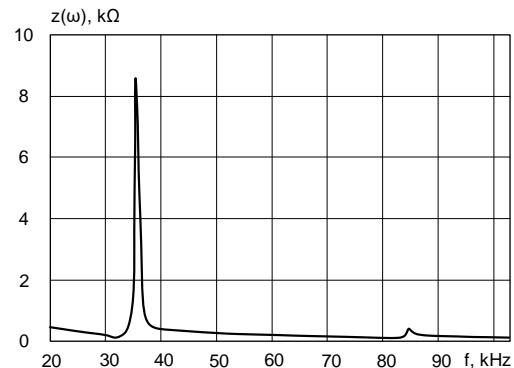


**Figure 6.** Electrical impedance of the piezoelectric disk in the mid-frequency area

When comparing the results of mathematical modelling of the electrical impedance of a piezoelectric disk in the region of medium frequencies (Fig. 4), and the results of experimental measurements (Fig. 6), it can be seen that the

obtained estimate is in good agreement with the true value of the electrical impedance. In this case, the frequency  $f = 15,25\text{kHz}$  corresponds to the value  $\Omega = \lambda R = 1$ .

**5. Results**

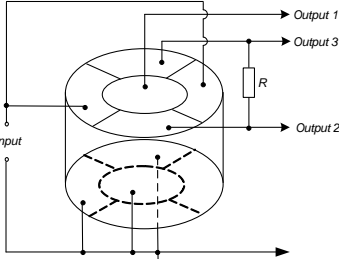
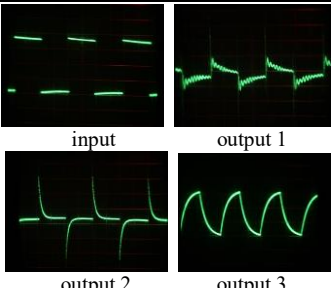
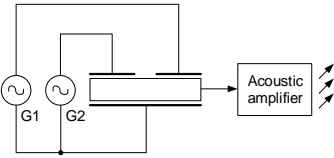
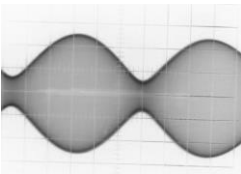
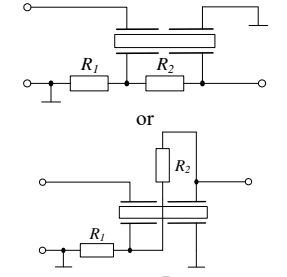
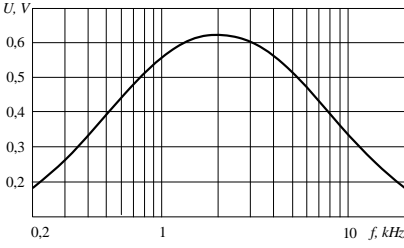
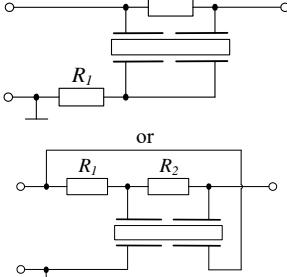
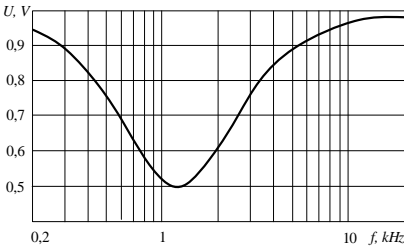
When designing piezoelectric transducers, a piezoelectric element of a certain shape and size from a certain piezoceramic material with certain electrophysical properties (characteristics) is usually used. In this case, only one transducer with certain characteristics (resonant frequency, sensitivity, etc.) can be obtained from a certain piezoelectric element. Therefore, the proposal to take into account the mutual arrangement of the vectors  $F$ ,  $P$  and  $E$  when developing the designs of transducers was an extraordinary and unusual decision. Such a mutual arrangement of vectors was called the spatial power structure of piezoelectric element. For example, in order to increase the level of sound pressure created using monomorphic piezoelectric elements, it was proposed to create an electric field in the transducer so that the electric

field vector  $E$  of the excitation voltage makes an angle  $\alpha$  with the polarization vector  $P$ , and  $0 < \alpha \leq 90^\circ$  [13].

Based on modelling the authors have developed methods for modifying disk piezoelectric transducers by using a polyelectrode design, technology of additional elements and the spatial power structure of piezoelectric transducers, as well as physical models of transducers based on multisectional piezoelectric disks with improved characteristics (Table 1).

Table 1 shows a designed multifunctional piezoelectric transducer with five electrodes located on the surfaces of the piezoelectric element and oscillograms of signals at its input and outputs (position 1). The bottom electrodes are projections of the top ones. The described version of the piezoelectric transducer, which allows processing the input signal, is, of course, not the only one. Changing the size of the electrodes, their relative position allows one to influence the parameters of the output signals and opens up wide opportunities for the design of piezoelectric transducers for critical application systems.

**Table 1.** Designed multisectional piezoelectric transducers

No.	Transducer circuit	Output characteristic
1		
2		
3		
4		

\* circuit 3 ( $R_1 = 12,6\text{ k}\Omega$ ,  $R_2 = 10,2\text{ k}\Omega$ ), circuit 4 ( $R_1 = 9,5\text{ k}\Omega$ ,  $R_2 = 38\text{ k}\Omega$ )

The developed electroacoustic radiator based on a piezoelectric adder with two systems of electrodes and the process of interference of two oscillations are presented in Table 1 (position 2). One system of electrodes is supplied with an electric voltage from the first generator, and the frequency of oscillations of the electric voltage of this generator is set equal to or close to one of the resonant frequencies of the piezoelectric element. The second system of electrodes of the piezoelectric element is supplied with voltage from the second generator. The oscillation frequency of this generator is also set close to the same resonant frequency so that the difference between the oscillation frequencies of the first and second generators is equal to the operating frequency of the radiator. Therefore, by exciting the transducer at inaudible frequencies, one can get an audio frequency at the output.

To expand the working range, piezoelectric elements can be included in the circuits of electrical filters. One of the disadvantages of such transducers is the need to use two piezoelectric elements or a piezoelectric element and a capacitor. To eliminate this disadvantage, the piezoelectric elements with separated electrodes can be used in the transducer circuits. The developed transducer with separated electrodes in a band-pass filter circuit as well as the transducer with separated electrodes in the band-stop filter circuit and their amplitude-frequency characteristics are indicated in Table 1 (positions 3 and 4) respectively. The piezoelectric transducer based on a disk piezoelectric element  $\varnothing 66 \times 3$  mm made of PZT type material was used for research.

## Conclusions

Physical processes in multisectional disk piezoelectric transducer were considered. The mathematical model of a multisectional disk piezoelectric transducer was built taking into account the acoustic feedback that exists between the area under the electrode of the primary electrical circuit and all, including the areas located under the electrodes of the secondary circuits. Proposed scheme maintains its logical structure in the wide range of the number of sections. The features of constructing mathematical models of multisectional transducers that arise when the sections are switched on in groups were considered. A comparative analysis of mathematically calculated and experimentally obtained values of the electrical impedance of the oscillating piezoceramic transducer revealed high convergence between them. Based on the modeling, the methods for modifying disk piezoelectric transducers using a polyelectrode design, technology of additional elements, the spatial power structure of piezoelectric transducers, and the physical models of transducers based on multisectional piezoelectric disks with improved characteristics, were designed.

## References

[1] Garsia Sespedes, N.V. Reliability of computer systems. *Mathematical machines and systems*, 2016, no. 4, pp. 146–151.

- [2] Li, J. Design of Active Vibration Control System for Piezoelectric Intelligent Structures. *International Journal of Education and Management Engineering (IJEME)*, 2012, vol. 2, no. 7, pp. 22–28. doi: 10.5815/ijeme.2012.07.04
- [3] Petrishchev, O. N., Bazilo, C. V. Principles and methods of mathematical modelling of oscillating piezoelectric elements. *Gordienko Publ., Cherkasy*, 2019.
- [4] Carazo, A.V. Piezoelectric Transformers: An Historical Review. *Actuators*, 2016, vol. 5, no. 12. doi:10.3390/act5020012
- [5] Fraden, J. *Handbook of Modern Sensors*. Springer, New York, 2010.
- [6] Barrett, S.F., Pack, D.J. *Embedded systems design and applications with the 68HC12 and HCS12*. Pearson/Prentice Hall, Upper Saddle River, NJ, 2005.
- [7] Kachapi, S. H. H. Nonlinear Vibration and Frequency Analysis of Functionally Graded- Piezoelectric Cylindrical Nano-shell with Surface Elasticity. *JJMIE*, vol. 12, no. 4, pp. 293–312.
- [8] Ebrahimi, F., Barati, M. R. Buckling Analysis of Nonlocal Embedded Shear Deformable Functionally Graded Piezoelectric Nanoscale Beams. *JJMIE*, vol. 11, no. 2, pp. 79–95.
- [9] Vavilov, V.D., Timoshenkov, S.P., Timoshenkov, A.S. *Microsystem sensors of physical quantities*. Technosfera, Moscow, 2018.
- [10] Bazilo, C. Modelling of bimorph piezoelectric elements for biomedical devices. In: Hu Z., Petoukhov S., He M. (eds) *Advances in Artificial Systems for Medicine and Education III. AIMEE 2019. Advances in Intelligent Systems and Computing*, 2020, vol. 1126. Springer, Cham, 2020, pp. 151–160. doi: 10.1007/978-3-030-39162-1\_14
- [11] Bazilo, C., Usyk, L. Modelling of Piezoelectric Disk Transducers Operated on Non-axisymmetric Oscillations for Biomedical Devices. In: Hu Z., Petoukhov S., He M. (eds) *Advances in Artificial Systems for Medicine and Education IV. AIMEE 2020. Advances in Intelligent Systems and Computing*, 2021, vol. 1315. Springer, Cham, 2021, pp. 191–200. doi: [https://doi.org/10.1007/978-3-030-67133-4\\_18](https://doi.org/10.1007/978-3-030-67133-4_18)
- [12] Buchacz, A., Placzek, M., Wróbel, A. Modelling of passive vibration damping using piezoelectric transducers – the mathematical model. *Maintenance and reliability*, 2014, vol. 16, no. 2, pp. 301–306.
- [13] Livingston, D., Kumar, K. P., Venugopal, N. Modelling and simulation of multiple piezoelectric transformer converters. *International Journal of Emerging Technology and Advanced Engineering*, 2013, vol. 3, no. 8, pp. 237–245.
- [14] Medianyuk, V. V., Bondarenko, Yu. Yu., Bazilo, C. V., Bondarenko M. O. Research of current-conducting electrodes of elements from piezoelectric ceramics modified by the low-energy ribbon-shaped electron stream. *Journal of Nano- and Electronic Physics*, 2017, vol. 10, issue 6, pp. 06012–1–06012–6. doi: 10.21272/jnep.10(6).06012
- [15] Bazilo, C., Zagorskis, A., Petrishchev, O., Bondarenko, Y., Zaika, V., Petrushko, Y. Modelling of Piezoelectric Transducers for Environmental Monitoring. In: *Proceedings of 10th International Conference "Environmental Engineering"*, Vilnius Gediminas Technical University, Lithuania, 2017. doi: 10.3846/enviro.2017.008
- [16] Petrishchev, O. N., Bazilo, C. V. Methodology of Determination of Physical and Mechanical Parameters of Piezoelectric Ceramics. *Journal of Nano- and Electronic Physics*, 2017, vol. 9, issue 3, pp. 03022–1–03022–6. doi: 10.21272/jnep.9(3).03022

## Appendix A

$$\Psi_1(k, R) = \frac{2K_{31}^2}{kR_1^{(2)}D_0} J_1(kR_1^{(2)}) \left[ M_1^{(2)} + N_1^{(8,10)} - \Psi_3(k, R)N_1^{(4,6)} - \Psi_7(k, R)N_1^{(12,14)} \right]; \quad (\text{A.1})$$

$$\begin{aligned} \Psi_5(k, R) = & \frac{2K_{31}^2}{kR_5^{(6)}D_0 \left[ 1 - \left( R_5^{(4)}/R_5^{(6)} \right)^2 \right]} \left\{ J_1(k, R_5^{(4)}, R_5^{(6)}) \left[ -M_8^{(2)} + N_8^{(8,10)} - \right. \right. \\ & \left. \left. - \Psi_3(k, R)N_8^{(4,6)} - \Psi_7(k, R)N_8^{(12,14)} \right] + N_1(k, R_5^{(4)}, R_5^{(6)}) \times \right. \\ & \left. \times \left[ M_9^{(2)} + N_9^{(8,10)} - \Psi_3(k, R)N_9^{(4,6)} - \Psi_7(k, R)N_9^{(12,14)} \right] \right\}; \quad (\text{A.2}) \end{aligned}$$

in which  $K_{31}^2$  is a square of the electromechanical coupling coefficient for the radial vibration mode in a thin piezoceramic disk;  $M_j^{(l)}$  is an algebraic complement that is obtained from the matrix  $M_0$  by striking out  $j$ -th row and  $l$ -th column;

$$\begin{aligned} N_1^{(4,6)} = & -M_1^{(4)} + M_1^{(6)}; \quad N_1^{(8,10)} = -M_1^{(8)} + M_1^{(10)}; \quad N_1^{(12,14)} = -M_1^{(12)} + M_1^{(14)}; \quad N_{4n}^{(4,6)} = M_{4n}^{(4)} - M_{4n}^{(6)}; \quad N_{4n}^{(8,10)} = M_{4n}^{(8)} - M_{4n}^{(10)}; \\ N_{4n}^{(12,14)} = & M_{4n}^{(12)} - M_{4n}^{(14)}; \quad N_{4n+1}^{(4,6)} = -M_{4n+1}^{(4)} + M_{4n+1}^{(6)}; \quad N_{4n+1}^{(8,10)} = -M_{4n+1}^{(8)} + M_{4n+1}^{(10)}; \\ N_{4n+1}^{(12,14)} = & -M_{4n+1}^{(12)} + M_{4n+1}^{(14)}; \end{aligned}$$

$D_0$  is the determinant of the strip matrix  $M_0 = \|m_j^{(l)}\|$ , nonzero elements  $m_j^{(k)}$  ( $j$  is a row number;  $l$  is a column number) of which are concentrated in the vicinity of the diagonal drawn from the upper left corner to the lower right corner;

$$\Psi_3(k, R) = \frac{1}{D_2} \left\{ F_1^{(3)}(k, R) \left[ F_7^{(7)}(k, R) - 1 \right] - F_1^{(7)}(k, R) F_7^{(3)}(k, R) \right\}; \quad (\text{A.3})$$

$$\Psi_7(k, R) = \frac{1}{D_2} \left\{ F_1^{(7)}(k, R) \left[ F_3^{(3)}(k, R) - 1 \right] - F_3^{(7)}(k, R) F_1^{(3)}(k, R) \right\}; \quad (\text{A.4})$$

$$D_2 = \left[ F_3^{(3)}(k, R) - 1 \right] \left[ F_7^{(7)}(k, R) - 1 \right] - F_7^{(3)}(k, R) F_3^{(7)}(k, R); \quad (\text{A.5})$$

$$F_1^{(2n+1)}(k, R) = F_0^{(2n+1)} \left[ -J_1(k, R_{2n+1}^{(2n)}, R_{2n+1}^{(2n+2)}) M_{4n}^{(2)} + N_1(k, R_{2n+1}^{(2n)}, R_{2n+1}^{(2n+2)}) M_{4n+1}^{(2)} \right]; \quad (\text{A.6})$$

$$F_0^{(2n+1)} = \frac{2K_{31}^2 f_{2n+1}(\omega)}{\left\{ 1 - \left[ R_{2n+1}^{(2n)}/R_{2n+1}^{(2n+2)} \right]^2 \right\} k R_{2n+1}^{(2n+2)} D_0}; \quad (\text{A.7})$$

$$F_3^{(2n+1)}(k, R) = F_0^{(2n+1)} \left[ J_1(k, R_{2n+1}^{(2n)}, R_{2n+1}^{(2n+2)}) N_{4n}^{(4,6)} + N_1(k, R_{2n+1}^{(2n)}, R_{2n+1}^{(2n+2)}) N_{4n+1}^{(4,6)} \right]; \quad (\text{A.8})$$

$$F_5^{(2n+1)}(k, R) = F_0^{(2n+1)} \left[ J_1(k, R_{2n+1}^{(2n)}, R_{2n+1}^{(2n+2)}) N_{4n}^{(8,10)} + N_1(k, R_{2n+1}^{(2n)}, R_{2n+1}^{(2n+2)}) N_{4n+1}^{(8,10)} \right]; \quad (\text{A.9})$$

$$F_7^{(2n+1)}(k, R) = F_0^{(2n+1)} \left[ J_1(k, R_{2n+1}^{(2n)}, R_{2n+1}^{(2n+2)}) N_{4n}^{(12,14)} + N_1(k, R_{2n+1}^{(2n)}, R_{2n+1}^{(2n+2)}) N_{4n+1}^{(12,14)} \right]; \quad (\text{A.10})$$

where  $J_1(k, R_{2n+1}^{(2n)}, R_{2n+1}^{(2n+2)}) = J_1(kR_{2n+1}^{(2n+2)}) - R_{2n+1}^{(2n)} J_1(kR_{2n+1}^{(2n)}) / R_{2n+1}^{(2n+2)}$  and

$N_1(k, R_{2n+1}^{(2n)}, R_{2n+1}^{(2n+2)}) = N_1(kR_{2n+1}^{(2n+2)}) - R_{2n+1}^{(2n)} N_1(kR_{2n+1}^{(2n)}) / R_{2n+1}^{(2n+2)}$  are Bessel and Neumann functions of the first order.

### Appendix B

$$\Psi_1(k, R) = \frac{2K_{31}^2 J_1(kR_1^{(2)})}{kR_1^{(2)} D_0} \left[ M_1^{(2)} - \Psi_3(k, R) N_1^{(4,6)} - \Psi_5(k, R) N_1^{(8,10)} - \Psi_7(k, R) N_1^{(12,14)} \right]; \quad (\text{B.1})$$

$$\Psi_5(k, R) = \frac{i\omega Z_5 C_5^* q(\omega)}{1 + i\omega Z_5 C_5^* p(\omega)}; \quad (\text{B.2})$$

$$q(\omega) = \frac{C_3^*}{C_5^*} \beta_3 + \beta_5 + \frac{C_7^*}{C_5^*} \beta_7; \quad p(\omega) = \frac{C_3^*}{C_5^*} (\lambda_3 - 1) + \lambda_5 - 1 + \frac{C_7^*}{C_5^*} (\lambda_7 - 1); \quad (\text{B.3})$$

where  $C_{2n+1}^* = (\pi \chi_{33}^* / \alpha) \left[ \left( R_{2n+1}^{(2n+2)} \right)^2 - \left( R_{2n+1}^{(2n)} \right)^2 \right]$  is the electrical capacity of the  $(2n + 1)$ -th ring area of the disk ( $n = 1, 2, 3$ );

$C_1^* = \pi \left( R_1^{(2)} \right)^2 \chi_{33}^* / \alpha$ ;  $C_5^* = \pi \left[ \left( R_5^{(6)} \right)^2 - \left( R_5^{(4)} \right)^2 \right] \frac{\chi_{33}^*}{\alpha}$ ;  $\chi_{33}^*$  is a dielectric constant for planar mode.

$$\beta_{2n+1} = \frac{2K_{31}^2}{kR_{2n+1}^{(2n+2)} \left[ 1 - \left( R_{2n+1}^{(2n)} / R_{2n+1}^{(2n+2)} \right)^2 \right] D_0} \left[ -M_{4n}^{(2)} J_1(k, R_{2n+1}^{(2n)}, R_{2n+1}^{(2n+2)}) + M_{4n+1}^{(2)} N_1(k, R_{2n+1}^{(2n)}, R_{2n+1}^{(2n+2)}) \right]; \quad (\text{B.4})$$

$$\lambda_{2n+1} = \frac{2K_{31}^2}{kR_{2n+1}^{(2n+2)} \left[ 1 - \left( R_{2n+1}^{(2n)} / R_{2n+1}^{(2n+2)} \right)^2 \right] D_0} \left[ S_{4n} J_1(k, R_{2n+1}^{(2n)}, R_{2n+1}^{(2n+2)}) + S_{4n+1} N_1(k, R_{2n+1}^{(2n)}, R_{2n+1}^{(2n+2)}) \right]; \quad S_{4n} = N_{4n}^{(4,6)} + N_{4n}^{(8,10)} + N_{4n}^{(12,14)}; \quad (\text{B.5})$$

$$S_{4n+1} = N_{4n+1}^{(4,6)} + N_{4n+1}^{(8,10)} + N_{4n+1}^{(12,14)}. \quad (\text{B.6})$$